Sirenomelia in *Bmp7* and *Tsg* compound mutant mice: requirement for Bmp signaling in the development of ventral posterior mesoderm

Lise Zakin[1], Bruno Reversade[1], Hiroki Kuroda[1], Karen M. Lyons[2] and Eddy M. De Robertis[1,*]

[1]Howard Hughes Medical Institute, and Department of Biological Chemistry, University of California, Los Angeles, CA 90095-1662, USA
[2]Department of Orthopaedic Surgery, University of California, Los Angeles, CA 90095, USA
*Author for correspondence (e-mail: derobert@mednet.ucla.edu)

Accepted 21 March 2005

Development 132, 2489-2499
Published by The Company of Biologists 2005
doi:10.1242/dev.01822

Summary

Sirenomelia or mermaid-like phenotype is one of the principal human congenital malformations that can be traced back to the stage of gastrulation. Sirenomelia is characterized by the fusion of the two hindlimbs into a single one. In the mouse, sirens have been observed in crosses between specific strains and as the consequence of mutations that increase retinoic acid levels. We report that the loss of bone morphogenetic protein 7 (Bmp7) in combination with a half dose or complete loss of twisted gastrulation (Tsg) causes sirenomelia in the mouse. Tsg is a Bmp- and chordin-binding protein that has multiple effects on Bmp metabolism in the extracellular space; Bmp7 is one of many Bmps and is shown here to bind to Tsg. In *Xenopus*, co-injection of Tsg and Bmp7 morpholino oligonucleotides (MO) has a synergistic effect, greatly inhibiting formation of ventral mesoderm and ventral fin tissue. In the mouse, molecular marker studies indicate that the sirenomelia phenotype is associated with a defect in the formation of ventroposterior mesoderm. These experiments demonstrate that dorsoventral patterning of the mouse posterior mesoderm is regulated by Bmp signaling, as is the case in other vertebrates. Sirens result from a fusion of the hindlimb buds caused by a defect in the formation of ventral mesoderm.

Key words: Sirenomelia, Twisted gastrulation (Twsg1) , Bmp, Bmp4, Morpholino, Limb bud, TGFβ, Chordin, Dorsoventral patterning, Mouse, *Xenopus*

Introduction

Sirenomelia is a human developmental malformation that has been a source of enduring interest. The abnormal fetuses are characterized by the fusion of both legs into a single member (Geoffroy Saint-Hilaire, 1837; Kampmeier, 1927). Descriptions of sirenomelia in human fetuses can be traced back to the 16th and 17th centuries, although these first reports were still a mixture of reality and mythical imagination. In addition to the hindlimb deformity, sirenomelic fetuses display a single umbilical artery (instead of two) and atrophic, cystic or absent kidneys (Feller and Sternberg, 1931). Several mechanisms have been proposed to explain sirenomelia: (1) deficiencies in caudal mesoderm, (2) mechanical defects resulting from lateral compression by amniotic folds and (3) trophic defects due to a deficient blood supply in the posterior region (Padmanabhan, 1998; Sadler and Langman, 2004).

Gluecksohn-Schoenheimer and Dunn published the first study on sirens in the mouse, in these terms: ‘Animal with fused and more or less perfectly developed posterior extremities like those mythical beings supposedly representing hybrids of man and fish’ (Gluecksohn-Schoenheimer and Dunn, 1945). Until then, sirenomelia had not been described in any mammal except humans. These mouse sirens were found in crosses between parents carrying mutations at the *T*, *Fused* or *ur* loci, thus establishing that sirenomelia can have a genetic basis. The phenotype was not described again in the mouse until 1970 (Hoornbeek, 1970). More recently, two groups linked retinoic acid to sirenomelia in gene knockouts of the retinoic acid-degrading enzyme, CYP26 (Abu-Abed et al., 2001; Sakai et al., 2001). Here, we report the appearance of the siren phenotype in *Tsg*/*Bmp7* compound mutants.

Dorsoventral patterning in vertebrate and invertebrate embryos is determined by a gradient of Bmp activity controlled in the extracellular space by a network of secreted proteins. Tsg (Twsg1 – Mouse Genome Informatics) is one of these Bmp regulators and can act both to promote and inhibit Bmp activity. When Tsg forms a stable ternary complex with Bmp and Chordin (Chd), Bmp signaling is prevented (Oelgeschläger et al., 2000; Chang et al., 2001; Larrain et al., 2001; Ross et al., 2001; Scott et al., 2001). However, the presence of Tsg in the complex facilitates cleavage of Chd by the metalloprotease Tld, enabling Bmp to signal again, and thus promoting Bmp activity (Oelgeschläger et al., 2000; Larrain et al., 2001; Oelgeschläger et al., 2003a; Oelgeschläger et al., 2003b). *Tsg* loss-of-function experiments in several species have resulted in various phenotypes interpreted as pro-Bmp or anti-Bmp effects. In *Drosophila*, *Tsg* mutation results in the loss of the amnioserosa, a tissue that requires the highest levels of Bmp/Dpp activity (Mason et al., 1994), and absence of Tsg

also impairs Bmp/Dpp diffusion in the embryo (Eldar et al., 2002). In *Xenopus*, microinjection of *Tsg* antisense morpholino oligos (MO) has been proposed to cause phenotypes consistent with an increase in Bmp signaling (Blitz et al., 2003). In zebrafish, by contrast, knockdown of *Tsg* dorsalizes the embryo, indicating that Tsg has a pro-Bmp effect in development (Little and Mullins, 2004; Xie and Fisher, 2005). In the mouse, *Tsg* has been shown to play a role in thymus, foregut, craniofacial and skeletal differentiation; Tsg appears to be a Bmp antagonist during T-cell development, yet it increases Bmp activity in skeletal growth (Nosaka et al., 2003; Petryk et al., 2004; Zakin and De Robertis, 2004). In a genetic background in which $Tsg^{-/-}$ mutants do not display head malformations on their own, heterozygosity for a *Bmp4* null allele leads to craniofacial defects and holoprosencephaly. This genetic interaction suggests that, in mouse, Tsg acts as a pro-Bmp4, because in the absence of Tsg, half a dose of Bmp4 is insufficient for head development (Zakin and De Robertis, 2004).

Studies on Tsg have focused on interactions with Bmp4, but, as shown here, Tsg also binds to Bmp7. In *Xenopus*, *Tsg* and *Bmp7* were knocked down using antisense MO oligos; the injected embryos displayed tail truncations and loss of the ventral fin. In the mouse, we performed crosses between *Tsg* and *Bmp7* mutant lines (Dudley et al., 1995; Zakin and De Robertis, 2004). As *Bmp7* mutant mice are perinatal lethal (Dudley et al., 1995) and *Tsg* mutants are viable (Zakin and De Robertis, 2004), increased or new phenotypes could be readily scored in this experimental setting. We found that $Tsg^{-/-}$;$Bmp7^{-/-}$ and $Tsg^{+/-}$;$Bmp7^{-/-}$ compound mutants displayed sirenomelia. The appearance of this rare, severe developmental phenotype revealed that in the absence of *Bmp7*, two functional alleles of *Tsg* are required for dorsoventral patterning of posterior mesoderm in mammals.

Materials and methods

Mouse strains and genotyping

Mice carrying the *Tsg* mutation (Zakin and De Robertis, 2004) were crossed to the *Bmp7* mutant strain (Dudley et al., 1995) and backcrossed into the hybrid strain B6SJL/F1 (Jackson Laboratories). Genotyping of pups or embryos was performed as described (Dudley et al., 1995; Zakin and De Robertis, 2004).

Mouse in situ hybridization, histology and skeletal preparations

Mouse in situ hybridization on whole mounts were performed (Henrique et al., 1995) using the following probes: *Bmp4* (Winnier et al., 1995), *Bmp7* (Lyons et al., 1995), brachyury (*T*) (Herrmann et al., 1990), *Fgf8* (Crossley and Martin, 1995), *Shh* (McMahon et al., 1998), *Tsg* (Zakin and De Robertis, 2004) and *Wnt3a* (Roelink and Nusse, 1991). Procedures for Alcian Blue and Alizarin Red skeletal staining (Belo et al., 1998), and β-gal staining of whole embryos (Zakin and De Robertis, 2004) were as described.

Western blot analysis

Immunoprecipitation of pure recombinant human Bmp7, TGFβ2 and Bmp4 (from R&D Systems) was performed as described (Oelgeschläger et al., 2000), using mouse Tsg-Flag pre-bound to anti-Flag agarose beads (M2, Sigma). Secreted proteins for crosslinking studies were harvested from conditioned medium from 293T cells transfected with human Tsg-HA (Tsg containing a hemagglutinin epitope tag at the C-terminus) or mouse Tsg-Flag (Flag epitope tag at the N-terminus), or human Bmp7. Before chemical crosslinking, samples were dialyzed into PBS, then incubated together and treated with DSS (disuccinimidyl suberate) as previously described (Oelgeschläger et al., 2000; Larrain et al., 2001). An immunopurified goat antibody specific for human Bmp7 (R&D systems) was used for western blot analyses.

Tsg-MO and Bmp7-MO injections and in situ hybridization

Xenopus microinjection and in situ hybridization were performed as described (Piccolo et al., 1997). Tsg-MO was as previously described (Blitz et al., 2003). Bmp7-MO sequence is as follows 5′-TTA-CTGTCAAAGCATTCATTTTGTC-3′ (underline indicates AUG start codon) and was designed using sequences identical in the two pseudo-alleles (Heasman et al., 2000; Oelgeschläger et al., 2003b). In vitro, Bmp7-MO efficiently and specifically inhibited translation of *Xenopus* Bmp7 mRNA (B.R., E.M.D.R. et al., unpublished). Tsg-MO (6 ng per embryo) or of Bmp7-MO (12 ng per embryo) were injected.

Ventral marginal zone (VMZ) assay and RT-PCR

VMZ explants from stage 10 embryos were cultured in 1× Steinberg solution until tailbud stage 20 and processed for RT-PCR or phenotypical analysis. The conditions and primer sequences were as described (http://www.hhmi.ucla.edu/derobertis).

Results

Tsg and Bmp7 bind to each other and have overlapping expression domains

Tsg is known to interact biochemically and genetically with Bmp4 (Oelgeschläger et al., 2000; Zakin and De Robertis, 2004). To test whether Tsg could also interact directly with Bmp7, we analyzed their biochemical interaction by co-immunoprecipitation and chemical crosslinking with DSS (Fig. 1A,A′). For co-immunoprecipitation, mouse Tsg-Flag pre-bound to agarose beads was incubated with 15 nM human recombinant Bmp7, with or without the addition of recombinant TGFβ2 or Bmp4 (Fig. 1A). Tsg was able to pull down Bmp7, and this binding was specific because it was not affected by a six-fold excess of TGFβ2. Bmp4 in equimolar amounts was able to reduce Bmp7 binding by about half, suggesting that Tsg binds both Bmps with comparable affinities (Fig. 1A, compare lanes 2 and 4). When Tsg and Bmp7 proteins from 293T cell culture supernatants were incubated together and chemically crosslinked (see Materials and methods), a bimolecular complex corresponding to a homodimer of Tsg bound to a homodimer of Bmp7 was formed (Fig. 1A′, lane 3).

Tsg and *Bmp7* expression domains overlapped in multiple tissues during embryogenesis (Fig. 1B-D′). In particular, histological sections showed that *Tsg* and *Bmp7* are co-expressed in ventral mesoderm and endoderm (Fig. 1E-G). The expression patterns of *Bmp7* and *Tsg* have been reported previously (Solloway and Robertson, 1999; Graf et al., 2001). At 8.25 dpc, *Tsg* and *Bmp7* were expressed diffusely in axial mesoderm and lateral mesoderm, gut endoderm and allantois (Fig. 1B,B′,E). At later stages, co-expression persisted in gut endoderm and overlapping or adjacent expression domains were found in limb bud mesenchyme, optic and otic vesicles, first branchial arch and posterior ventral mesoderm (Fig. 1C,C′,D,D′,F,G).

We conclude that Tsg and Bmp7 proteins are capable of establishing direct biochemical interactions, and that the

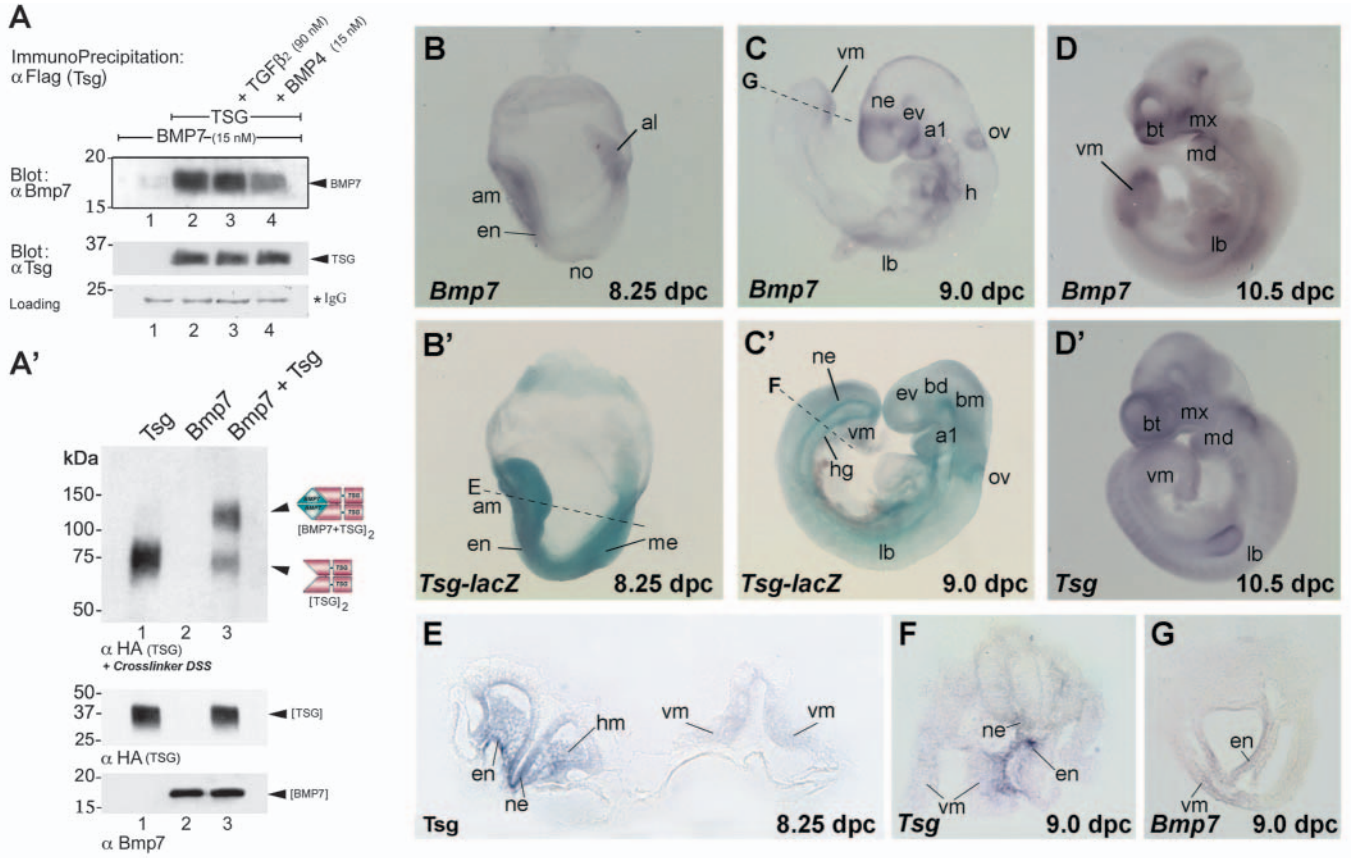

Fig. 1. Tsg and Bmp7 interact biochemically and are expressed in overlapping domains. (A) Bmp7 co-immunoprecipitates with Tsg. Top panel was probed with an anti-Bmp7 antibody. Bmp7 was pulled down only in the presence of Tsg (compare lanes 1 and 2). This Tsg/Bmp7 interaction was not competed by a sixfold excess of TGFβ2 (lane 3) but was partially competed by equimolar amounts of Bmp4 (lane 4). Middle panel provides a control for the amount of Tsg immunoprecipitated; the bottom panel serves as a loading control for antibodies on the beads. (A′) Crosslinking of Tsg and Bmp7 proteins by DSS. A bimolecular complex of Tsg and Bmp7 is formed in lane 3. Tsg protein is HA tagged. Top panel (crosslinked) and middle panel (no crosslinker) were probed with an anti-HA antibody; bottom panel (no crosslinker) was probed with anti-Bmp7 antibody. Tsg protein forms a homodimer when crosslinked (lane 1, top panel). In the presence of Bmp7 (lane 3, top panel) a bimolecular complex (consistent with a homodimer of Tsg binding a homodimer of Bmp7) runs around 110 kDa. (B-D′) Expression of *Tsg* and *Bmp7* analyzed by whole-mount in situ hybridization and β-gal staining. (B,B′) *Bmp7* and *Tsg* are co-expressed in allantois (al), axial and lateral mesoderm (am) and gut endoderm (en) at 8.25 dpc. *Tsg* expression is visualized via an in-frame fusion to *lacZ*. (C,C′) At 9.0 dpc, *Tsg* and *Bmp7* are found in gut endoderm, branchial arch one (a1), eye vesicle (ev) and otic vesicle (ov). (D,D′) At 10.5 dpc, *Tsg* and *Bmp7* are co-expressed in posterior ventral mesoderm (vm), limb bud (lb), first pharyngeal arch and basal telencephalon (bt). (E,F) Sections of 8.25 and 9.0 dpc embryos showing *Tsg* mRNA in endoderm, neurectoderm, head mesenchyme (hm) and ventral mesoderm (vm). (G) Section of a 9.0 dpc embryo showing expression of *Bmp7* in ventral mesoderm and endoderm of the hindgut. Plane of sections are indicated in B′,C,C′. h, heart; hg, hindgut; me, mesoderm; md, mandibular component of first pharyngeal arch; mx, maxillary component of first pharyngeal arch; ne, neuroectoderm; no, node.

two genes share overlapping expression domains during embryogenesis. To investigate whether genetic interactions existed, we next crossed mice carrying mutations in the *Tsg* and *Bmp7* genes (Dudley et al., 1995; Zakin and De Robertis, 2004).

Sirenomelia and embryonic lethality in *Tsg*$^{-/-}$;*Bmp7*$^{-/-}$ and *Tsg*$^{+/-}$;*Bmp7*$^{-/-}$ compound mutants

Tsg and *Bmp7* mutant strains were mated to generate *Tsg;Bmp7* double heterozygotes. Table 1 summarizes the results obtained from a total of 197 neonates from *Tsg*$^{+/-}$;*Bmp7*$^{+/-}$ intercrosses. Interestingly, only 0.5% (n=1) of *Tsg*$^{-/-}$;*Bmp7*$^{-/-}$ mutants and 2.5% (n=5), of *Tsg*$^{+/-}$;*Bmp7*$^{-/-}$ mutants were observed, instead of the expected 6.25% and 12.5%, respectively. This suggested embryonic lethality associated with these genotypes. Embryonic lethality required the loss of both copies of *Bmp7*; for example, the number of *Tsg*$^{-/-}$;*Bmp7*$^{+/-}$ mutants recovered was normal (Table 1). Phenotypes previously known to occur when only *Bmp7* is mutated (microphthalmia, hindlimb polydactyly, sternebral defects) (Dudley et al., 1995) were examined, and most appeared enhanced in *Tsg*$^{-/-}$;*Bmp7*$^{-/-}$ and *Tsg*$^{+/-}$;*Bmp7*$^{-/-}$ animals (Table 1). Two of these neonates displayed a striking sirenomelia phenotype, characterized by the presence of a single hindlimb. Examination of embryos recovered between 9.5 dpc and 12.5 dpc confirmed that all 23 cases with clear sirenomelia had either the *Tsg*$^{+/-}$;*Bmp7*$^{-/-}$ or *Tsg*$^{-/-}$;*Bmp7*$^{-/-}$ genotypes. These results indicate that in the absence of *Bmp7* there is a dose-dependent requirement of *Tsg* for mouse development.

Table 1. Characterization of neonates obtained from *Tsg*$^{+/-}$;*Bmp7*$^{+/-}$ intercrosses

Genotype	Neonates	Expected percentage	Observed percentage	Anophthalmia microphthalmia (%)	Hindlimd polydactyly* (%)	Sirenomelia (%)	Sternebral defects (%)*
Tsg$^{+/+}$;*Bmp7*$^{+/+}$	18	6.25	9	0	N/A	0	N/A
Tsg$^{+/+}$;*Bmp7*$^{+/-}$	37	12.5	19	0	N/A	0	N/A
Tsg$^{+/-}$;*Bmp7*$^{+/-}$	55	25	28	0	N/A	0	N/A
Tsg$^{+/-}$;*Bmp7*$^{+/+}$	30	12.5	15	0	N/A	0	N/A
Tsg$^{-/-}$;*Bmp7*$^{+/+}$	12	6.25	6	0	N/A	0	N/A
Tsg$^{-/-}$;*Bmp7*$^{+/-}$	28	12.5	14	0	N/A	0	N/A
Tsg$^{+/+}$;*Bmp7*$^{-/-}$	11	6.25	6	9 (82%)	2 (18%)	0	5 (45%)
Tsg$^{+/-}$;*Bmp7*$^{-/-}$	5	12.5	2.5	5 (100%)	4 (80%)	1 (20%)	4 (80%)
Tsg$^{-/-}$;*Bmp7*$^{-/-}$	1	6.25	0.5	1 (100%)	1 (100%)	1 (100%)	1 (100%)
Total	197						

N/A, not assessed.
*Determined by skeletal staining.

The sirenomelia phenotype can be seen in Fig. 2. In ventral view, a single medial hindlimb was present in pups that had otherwise normal forelimbs (Fig. 2A,B). Alcian blue/Alizarin red staining of the skeletons of *Tsg*$^{-/-}$;*Bmp7*$^{-/-}$ and *Tsg*$^{+/-}$;*Bmp7*$^{-/-}$ pups showed that the single lower limb consisted of the fusion of two independent hindlimbs (Fig. 2C-F). Most skeletal elements were duplicated, but the two limbs were fused at the pelvis and at the heel of the foot (Fig. 2F), and lacked the fibula. The *Tsg*$^{-/-}$;*Bmp7*$^{-/-}$ mutant had only one foot (designated sympus monopus) (Kampmeier, 1927) with only five digits and a bifurcation of the first digit (Fig. 2D; inset). The *Tsg*$^{+/-}$;*Bmp7*$^{-/-}$ mutant had two fused feet (sympus dipus) (Kampmeier, 1927) with nine digits, a single first digit and a bifurcation of one of the second digits (Fig. 2F; inset). The sirenomelia phenotype in the *Tsg*$^{-/-}$;*Bmp7*$^{-/-}$ neonate is considered more severe due to the presence of only one foot. The tail was shorter, with fewer vertebrae and delayed and reduced bone deposition with respect to the wild-type (Fig. 2C,D). As Bmps and Tsg promote chondrogenesis and bone deposition, this is consistent with the notion that the compound mutants have less Bmp signaling. The thoracic region was also affected in *Tsg*$^{-/-}$;*Bmp7*$^{-/-}$ and *Tsg*$^{+/-}$;*Bmp7*$^{-/-}$ mutants (see Fig. S1 in the supplementary material).

In conclusion, the analysis of the skeletons of *Tsg*$^{-/-}$;*Bmp7*$^{-/-}$ and *Tsg*$^{+/-}$;*Bmp7*$^{-/-}$ mutants revealed phenotypes indicative of reduced Bmp signaling, not observed in either mutant alone. These results suggest that in a *Bmp7*-null background the lack, or haploinsufficient doses, of Tsg affects the activity of other Tsg-interacting Bmps, which in vivo would be

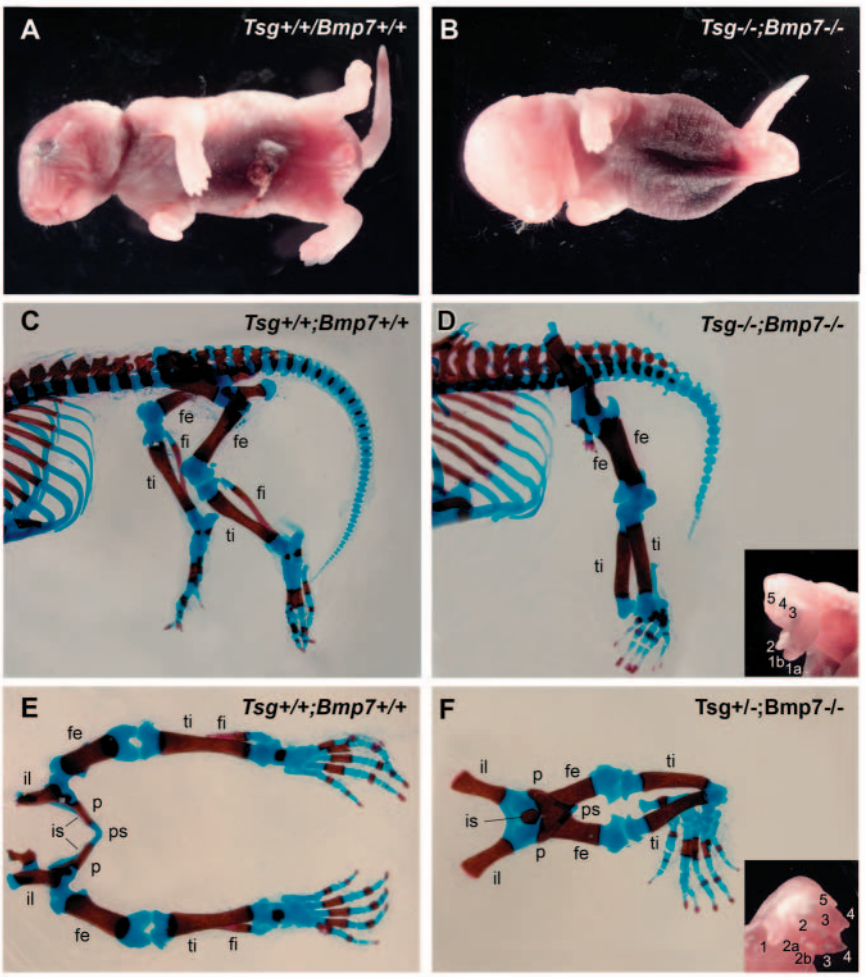

Fig. 2. Sirenomelia in *Tsg*$^{-/-}$;*Bmp7*$^{-/-}$ and *Tsg*$^{+/-}$;*Bmp7*$^{-/-}$ compound mutants. (A,B) Comparison of a wild-type neonate with a *Tsg*$^{-/-}$;*Bmp7*$^{-/-}$ mutant displaying sirenomelia. The mutant appears normal up to the level of the hindlimbs which are fused. (C-F) Alcian Blue (cartilage) and Alizarin Red (bone) preparations of wild-type and *Tsg*$^{-/-}$;*Bmp7*$^{-/-}$ and *Tsg*$^{+/-}$;*Bmp7*$^{-/-}$ mutants. (C,D) Lateral view of the posterior region of a wild-type and *Tsg*$^{-/-}$;*Bmp7*$^{-/-}$ skeleton. In the mutant, the tail is shorter and has fewer vertebrae. The single hindlimb contains two femurs (fe), two tibias (ti), a single foot and lacks both fibulae (fi). (E,F) Ventral views of the hindlimbs and pelvic region of a wild-type and *Tsg*$^{+/-}$;*Bmp7*$^{-/-}$ neonate. The mutant hindlimb is formed by the fusion of two hindlimbs at the level of the ischium (is); two feet are present, fused at the level of the heel. Insets in D and F show higher magnification views of the feet of *Tsg*$^{-/-}$;*Bmp7*$^{-/-}$ and *Tsg*$^{+/-}$;*Bmp7*$^{-/-}$ neonates, respectively. Digits are indicated by numbers and digit duplications by letters. il, ilium; is, ischium; p, pubic bone; ps, pubic symphysis.

functionally redundant with *Bmp7*. In *Bmp7*$^{-/-}$ embryos, these other Bmps would compensate for the loss of *Bmp7*; however, when Tsg function is reduced, the activity of these other Bmps is lowered to levels incompatible with normal development.

Knockdown of *Tsg* and *Bmp7* affects ventral development in *Xenopus* embryos

These interactions were also observed in *Xenopus* loss-of-function experiments using antisense MO oligonucleotides. Tsg-MO (Blitz et al., 2003) and Bmp7-MO, were injected independently and in combination, into *Xenopus* embryos (Fig. 3). Injections were performed at the site of *Tsg* and *Bmp7* expression, in the ventral side. Injection of Bmp7-MO at the four-cell stage produced a mild phenotype characterized by a partial loss of the ventral fin and a posteriorized anus (Fig. 3D,I,E,J; arrowhead in J). Similar injections of Tsg-MO produced a phenotype characterized by a bent tail and reduced ventral fin tissue (Fig. 3N,O). The ventral fin tissue is an indicator of ventral mesoderm development (Hammerschmidt and Mullins, 2002) and in *Xenopus* is derived from the ventral-most mesoderm (Tucker and Slack, 2004). At earlier stages, Tsg-MO or Bmp7-MO caused a reduction of the ventrally expressed gene sizzled (Fig. 3A,F,K), a marker of high Bmp signaling (Collavin and Kirschner, 2003; De Robertis and Kuroda, 2004). The anterior marker *Otx2*, which is negatively regulated by Bmp, was unaffected or slightly expanded by injection of the individual morpholinos (Fig. 3B,G,L). When Tsg-MO and Bmp7-MO were injected together, *sizzled* expression was almost completely eliminated, indicating a loss of Bmp signaling (Fig. 3P). *Otx2* expression domain was significantly expanded at the neurula stage, also indicating decreased Bmp signaling (Fig. 3Q). However, the head region marked by *Otx2* and somitic mesoderm marked by *Myod1* appeared normal by the early tailbud stage (Fig. 3R). When Bmp7-MO and Tsg-MO were co-injected, the ventral fin phenotype increased markedly, causing the development of tadpoles with a truncated tail and virtually no ventral fin (Fig. 3S,T).

One of the most sensitive assays for Bmp signaling levels is provided by the *Xenopus* ventral marginal zone (VMZ) explant (Fig. 4A). When such explants were prepared from embryos injected ventrally with Bmp7-MO or Tsg-MO, they resembled lateral marginal zone (LMZ) explants containing polarized patches of unpigmented cells (Fig. 4B-D). When Bmp7-MO and Tsg-MO were co-injected, the explants elongated and adopted the external appearance of dorsal marginal zone (DMZ) explants (Fig. 4E). As shown by the RT-PCR gene marker analyses of Fig. 4F, both Tsg-MO and Bmp7-MO had anti-Bmp effects in *Xenopus*. VMZ explants expressed the ventral mesodermal marker β-globin (lane 4), while Tsg-MO (lane 5) or Bmp7-MO (lane 9) expressed markers present in more lateral LMZ, explants (lane 3), such as *α-actin*, the neural crest marker *slug*, and the neuronal marker *N-tubulin*. When Tsg and Bmp7 were knocked down simultaneously (lane 8), strong induction of somitic mesoderm (*α-actin*), neurons (*N-tubulin*), cement gland (marked by *XAG*) and even the dorsal midline markers *pintallavis/HNF3β* and *sonic hedgehog* (*Shh*) was observed. This pattern of expression of dorsoventral markers in double knockdowns was very similar to that of uninjected DMZ (also known as Spemann organizer) explants

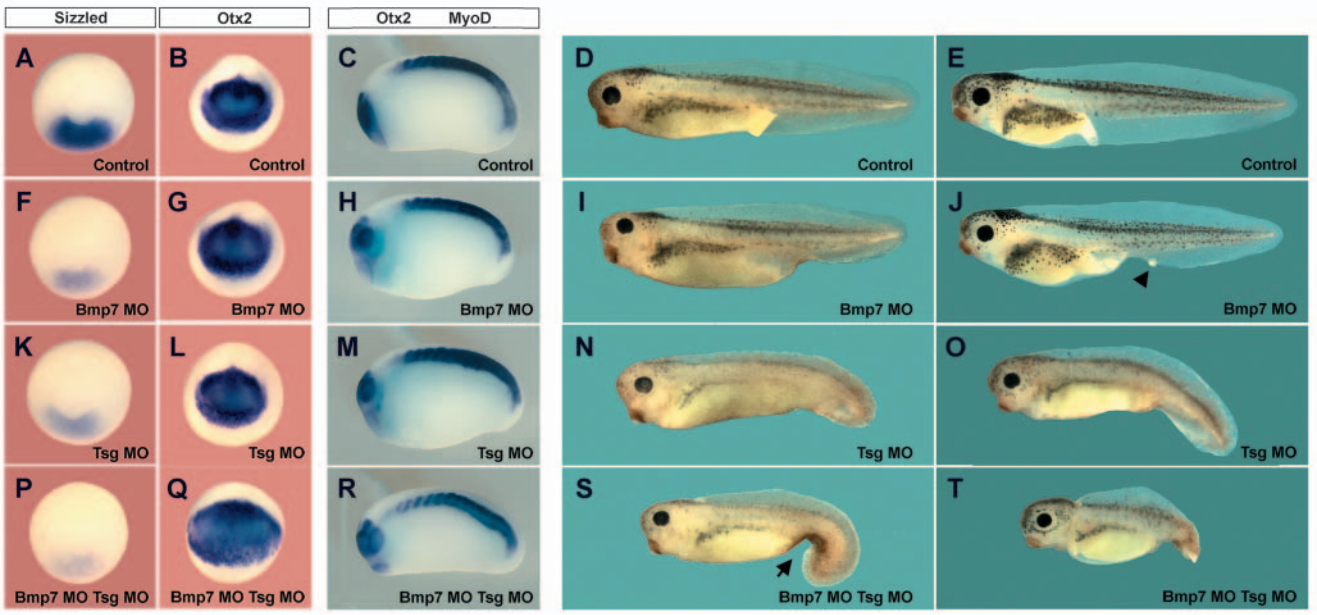

Fig. 3. *Tsg* and *Bmp7* cooperate in ventral development in *Xenopus* embryos. (A,F,K,P) Control and morpholino-injected embryos at stage 12 hybridized with *sizzled* probe. Expression of *sizzled* is reduced in Bmp7-MO- or Tsg-MO-injected embryos and almost completely lost in the Bmp7-MO/Tsg-MO-injected embryos. (B,G,L,Q) Expression of *Otx2* in injected embryos at stage 13; there is an increase in Bmp7-MO/Tsg-MO-injected embryos. (C,H,M,R) Embryos at stage 18 hybridized with *Otx2* and *Myod1* probes. The expansion of *Otx2* regulates and is no longer seen at this stage. (D,E,I,J,N,O,S,T) Phenotypes of morpholino-injected embryos at (D,I,N,S) stage 39 (2 day) and (E,J,O,T) stage 42 (3 day). Bmp7-MO-injected embryos have a reduced ventral fin (arrowhead); Tsg-MO-injected embryos have a bent tail and reduction of ventral fin. Co-injection of Bmp7-MO and Tsg-MO synergize, causing a severe loss of ventral fin (arrow in S) and at later stages truncation of the entire tail region (T).

(compare lanes 2 and 8). Importantly, we also injected several dosages of Bmp7-MO (lanes 6-8), showing that *Bmp7* and *Tsg* interacted also at intermediate *Bmp7* levels in *Xenopus* embryos. As the siren phenotype in mouse was only observed on a *Bmp7*$^{-/-}$ background, these epistatic experiments provide evidence that *Bmp7* and *Tsg* interact with each other in vivo.

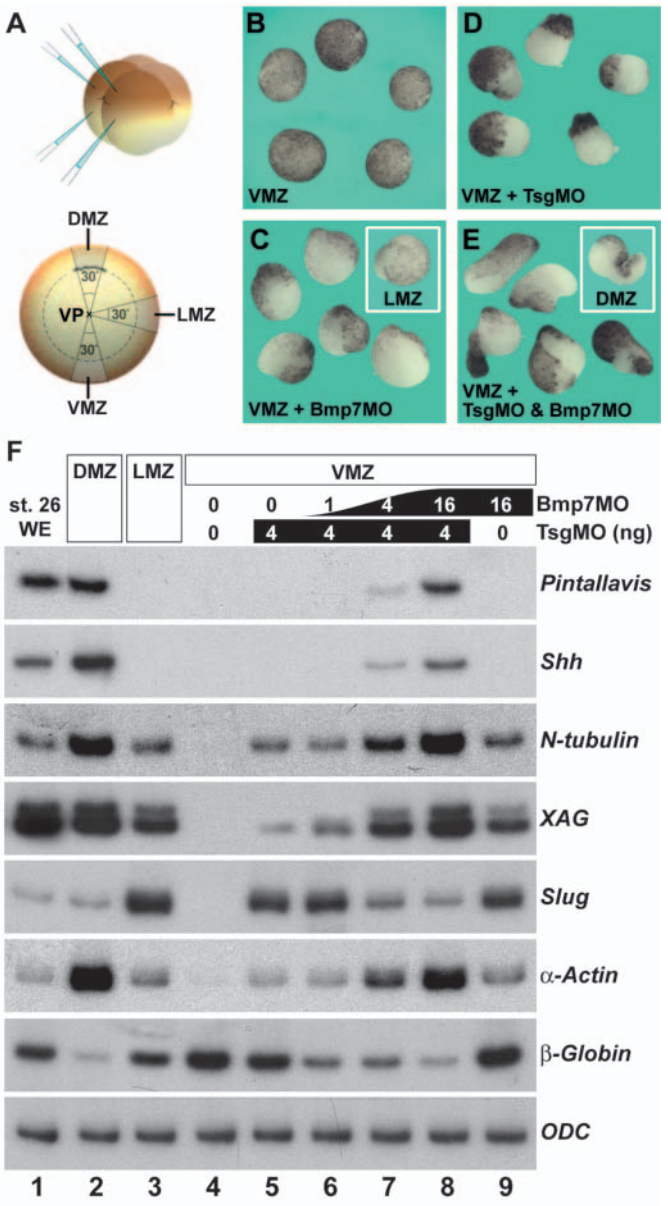

Fig. 4. VMZ explants co-injected with Tsg-MO and Bmp7-MO are strongly dorsalized and adopt the identity of DMZ explants. (A) Experimental design of the DMZ, LMZ and VMZ explants. (B) VMZs from wild-type embryos cultured until tailbud stage 20. (C) VMZs from Bmp7-MO-injected embryos are dorsalized and resemble LMZs (inset). (D) VMZs from Tsg-MO-injected embryos showing dorsalization (unpigmented regions). (E) VMZs from Tsg-MO- and Bmp7-MO-injected embryos elongate similarly to DMZ (Spemann organizer) explants (shown in the inset). (F) RT-PCR assays of stage 26 whole embryos (WE) (lane 1), DMZs (lane 2), LMZs (lane 3) and VMZs (lane 4) from uninjected embryos or from embryos injected with Tsg-MO (lane 5), Bmp7-MO (lane 9), with Tsg-MO or several doses of Bmp7-MO (lanes 6-8). VMZs from embryos injected with both MOs express the same markers as wild-type DMZ explants (compare lanes 2 and 8), indicating strong dorsalization and reduced Bmp signaling. VP, vegetal pole; WE, whole embryo.

These results show that the wild-type function of Tsg in *Xenopus* is to promote Bmp signaling, as is the case in zebrafish (Little and Mullins, 2004; Xie and Fisher, 2005). They also show that Bmp7 and Tsg cooperate in the formation of ventral tissues, suggesting that the siren phenotype observed in mouse could be due to a loss of Bmp signaling in ventral mesoderm.

Tsg$^{-/-}$*;Bmp7*$^{-/-}$ and *Tsg*$^{+/-}$*;Bmp7*$^{-/-}$ embryos lack ventral mesodermal structures

We next dissected embryos from *Tsg*$^{+/-}$*;Bmp7*$^{+/-}$ heterozygous matings at different stages. Most *Tsg*$^{-/-}$*;Bmp7*$^{-/-}$ and *Tsg*$^{+/-}$*;Bmp7*$^{-/-}$ compound mutants recovered after 9.5 dpc were found dead. The likely cause of lethality is related to defects in chorioallantoic fusion (discussed below). At 10.5 dpc, compound mutant embryos appeared developmentally delayed compared with their littermates (Fig. 5A-C). The morphology of embryos displaying sirenomelia, in which the hindlimb buds are fused along the ventral midline into a single bud is shown in Fig. 5B (arrow); this fusion can be best seen in ventral views such as the one shown in Fig. 7D′ below. We found that 100% of *Tsg*$^{-/-}$*;Bmp7*$^{-/-}$ (11 embryos out of a total of 140) and 75% of *Tsg*$^{+/-}$*;Bmp7*$^{-/-}$ (12 embryos) were abnormal. The siren phenotype was observed in 75% of *Tsg*$^{-/-}$*;Bmp7*$^{-/-}$ mutants and in 88% of *Tsg*$^{+/-}$*;Bmp7*$^{-/-}$ mutants. In addition, kinked neural tubes were often seen (data not shown). In rarer cases, 25% of *Tsg*$^{-/-}$*;Bmp7*$^{-/-}$ and 12% of *Tsg*$^{+/-}$*;Bmp7*$^{-/-}$ mutants were severely underdeveloped and displayed heart edema (Fig. 5C).

Serial histological sections were performed on 9.5 dpc embryos from the hindlimb bud region to the tip of the tail to examine the anatomy of embryos with sirenomelia (Fig. 5D-G′). At the level of the hindlimb buds in the normal embryos four blood vessels are seen. Two dorsal aortae, which after they curve back into the tailbud, form ventrally the recurved part of the distal aortae separating two distinct lateral coelomic cavities (Fig. 5D,E). Two thickenings of the lateral plate mesoderm mark the forming of the left and right hindlimb buds (Fig. 5E). In mutant embryos, a single coelomic cavity was observed (Fig. 5E′, see Fig. S2 in the supplementary material), and the recurved ventral region of the posterior aorta was absent (Fig. 5D′,E′, see Fig. S2 in the supplementary material). In compound mutants, the posterior arterial system had a single abnormally placed umbilical artery directly arising from the dorsal aorta (Fig. 5D′), and a single thickening of the mesoderm was seen in the ventral midline, marking the site of the fused hindlimb buds (Fig. 5E′). Most defects were ventral in *Tsg;Bmp7* compound mutants (Fig. 5F,F′; see Fig. S2 in the supplementary material) and, more posteriorly, tailbud mesoderm cells were sparser (Fig. 5G,G′). In summary, the sirenomelic phenotype is caused by a reduction of ventral mesodermal tissue that results in the fusion of the hindlimb buds and coelomic cavities. The results indicate a requirement in the mouse for Bmp signaling in ventral mesoderm formation and/or survival.

Onset of ventral defects in *Tsg*$^{-/-}$*;Bmp7*$^{-/-}$ and *Tsg*$^{+/-}$*;Bmp7*$^{-/-}$ compound mutants

To determine the onset of this ventroposterior mesodermal

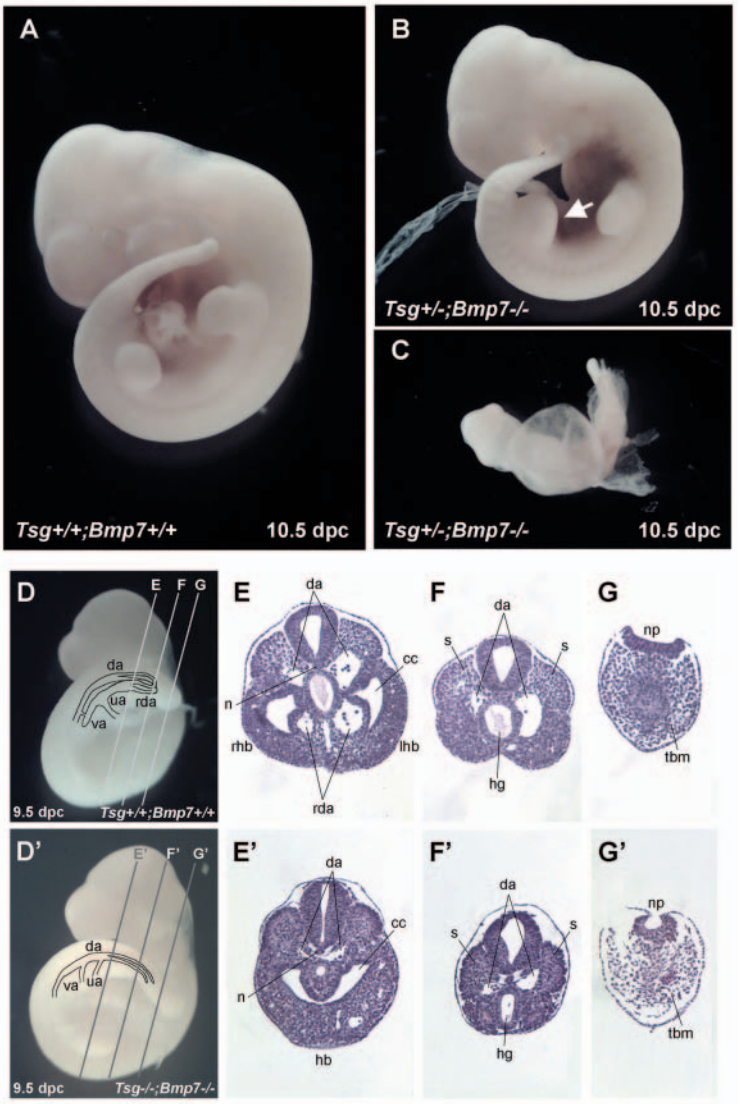

Fig. 5. Phenotypic abnormalities in $Tsg^{-/-};Bmp7^{-/-}$ and $Tsg^{+/-};Bmp7^{-/-}$ compound mutants in the mouse. (A) Wild-type embryo 10.5 dpc. (B) Side view of a $Bmp7^{-/-},Tsg^{-/-}$ mutant with sirenomelia; the hindlimb buds are fused into a single bud (arrow). (C) Ventral view of a severely affected $Tsg^{+/-};Bmp7^{-/-}$ mutant embryo with heart edema and underdeveloped anterior and posterior structures. (D-G′) Histological analyses of the posterior region of 9.5 dpc wild-type and $Tsg^{-/-};Bmp7^{-/-}$ embryos. (D,D′) Side view of the embryos indicating the level of sections in E-G′. The posterior arterial system is drawn schematically and superimposed; the dorsal aorta (da) curves ventrally in the tailbud, forming the recurved distal aorta (rda), from which the umbilical artery (ua) originates. (E-G′) Transverse serial sections of embryos shown in D and D′ stained with Hematoxylin and Eosin. (E,E′) Section at the level of the right and left hindlimb buds (rhb, lhb) showing the absence of the rda, fusion of the hindlimb buds (hb) and a single coelomic cavity (cc) in the mutant. (F,F′) More posterior sections showing a decreased diameter of the tail at the level of the aortic curvature. (G,G′) Section at the tip of the tail showing fewer tailbud mesoderm cells and a normal neural plate in the mutant. hg, hindgut; lhb, left hindlimb bud; n, node; nt, neural tube; rhb, right hindlimb bud; s, somite; tbm, tail bud mesoderm; ua, umbilical artery; va, vitelline artery.

phenotype, mesodermal markers were analyzed at 8.25 dpc and 9.0 dpc (Fig. 6). Brachyury is a notochord and primitive streak marker required for axial elongation and formation of posterior mesoderm (Herrmann et al., 1990; Wilson et al., 1995). Its expression was not significantly changed at 8.25 dpc (Fig. 6A,A′). *Fgf8* is required for cell migration and patterning of the primitive streak and the mesodermal cells exiting from it (Crossley and Martin, 1995; Sun et al., 1999) and for formation of posterior mesoderm (Draper et al., 2003). Its expression was reduced at 8.25 dpc in mutant embryos (Fig. 6B-C′). Expression of *Wnt3a*, which regulates paraxial mesoderm fates at the expense of neuroectodermal fates (Yoshikawa et al., 1997), was unchanged in the primitive streak and ectoderm (data not shown). Thus, at 8.25 dpc, mesodermal cells appear properly specified (as shown by the normal expression of brachyury and *Wnt3a*), but posterior mesoderm cells may be reduced in number, as suggested by the decrease in *Fgf8* staining.

After the embryo has turned at 9.0 dpc, most mutants displayed a small and poorly developed allantois delayed in its fusion to the chorion (Fig. 6E′,F′). At this stage, expression of *Brachyury* in tailbud mesoderm was moderately reduced in the ventral mesoderm close to the tip of the tail (Fig. 6D,D′). Normally at 9.0 dpc, *Bmp4* expression is found in posterior lateral plate mesoderm and extra-embryonic mesoderm of the allantois (Fujiwara et al., 2001). In mutant embryos, the *Bmp4* expressing region closest to the tip of the tail was reduced and the allantois failed to fuse to the chorion (Fig. 6E,E′).

We found that the onset of ventral mesoderm defects could be traced prior to the turning of the embryo and was initially characterized by a deficit in posterior mesoderm cells expressing *Fgf8*. Posterior mesodermal cells appear to be specified normally in the posterior primitive streak, but are unable to either proliferate or survive. The lack of ventral posterior mesoderm could also help explain the defects observed in allantoic growth and fusion to the chorion, as the allantois increases in size by the recruitment of cells from the posterior primitive streak (Fujiwara et al., 2001). The defect is not due to a failure of cells exiting the primitive streak as no ectopic neural structures were observed in $Tsg^{-/-};Bmp7^{-/-}$ and $Tsg^{+/-};Bmp7^{-/-}$ mutants, which would have indicated transformation of axial mesoderm into neural fates (Yoshikawa et al., 1997; Abu-Abed et al., 2001; Sakai et al., 2001). We conclude that *Tsg* and *Bmp7* appear to be required for the proper survival and/or proliferation of posterior ventral mesoderm cells and their derivatives.

Development of fused hindlimb bud territory in siren mutants

We next examined the development of the hindlimb buds and posterior ventral structures (Fig. 7). At 9.5 dpc *Bmp4* marks the ventrolateral part of the embryo in ectoderm, limb mesenchyme and lateral plate mesoderm (arrow in Fig. 7A) (Ahn et al., 2001). In $Tsg^{-/-};Bmp7^{-/-}$ embryos, *Bmp4* staining in limb bud mesoderm spans the embryo transversely (90° from the normal orientation of the hindlimb bud), while the ventralmost mesoderm forms a separate domain (Fig. 7A′,B′). The apical ectodermal ridge marker *Fgf8* (Crossley and

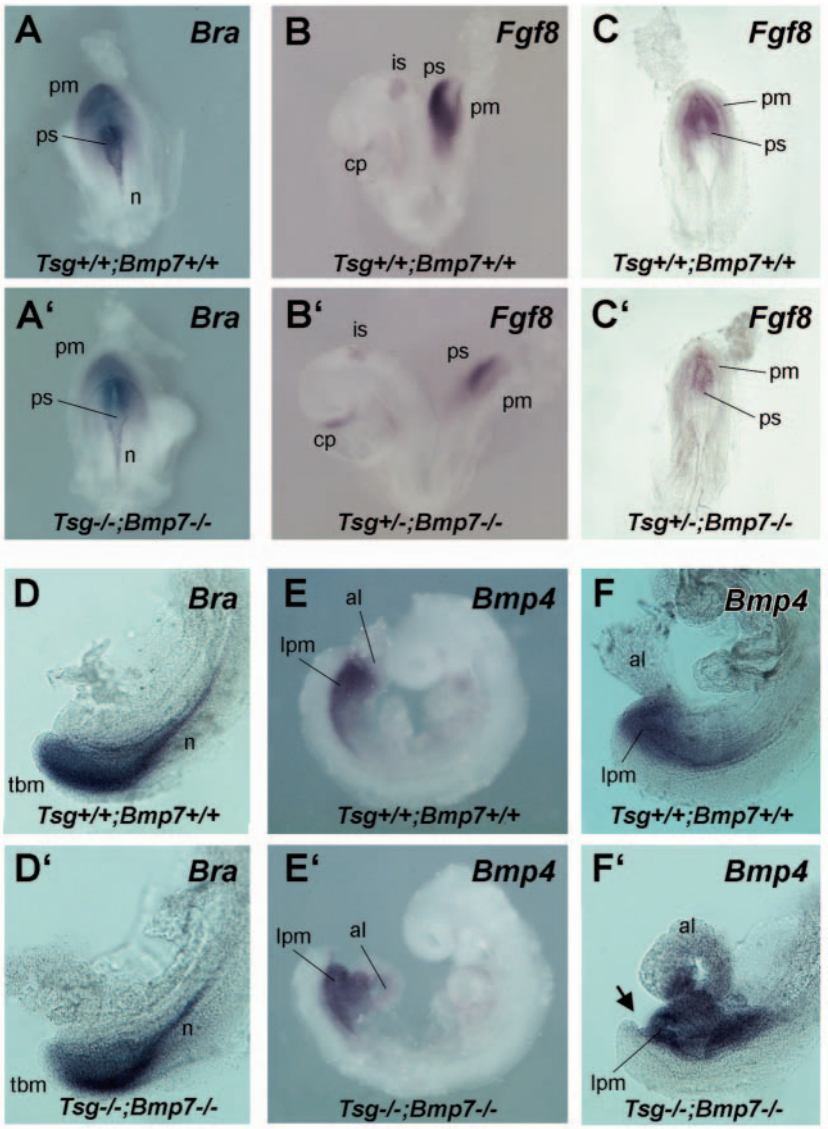

Fig. 6. Onset of ventral and posterior mesoderm defects in $Tsg^{-/-};Bmp7^{-/-}$ and $Tsg^{+/-};Bmp7^{-/-}$ compound mutants. (A,A′) Ventral view of posterior primitive streak (ps) region of wild-type and mutant embryos stained with brachyury. The expression of brachyury is unchanged at 8.25 dpc in the mutant. (B,B′) Side view of 8.25 dpc embryos before turning hybridized with *Fgf8*. Staining of the primitive streak and posterior mesoderm (pm) is fainter in the mutant. (C,C′) Dorsal view of the posterior region of embryos shown in B and B′, respectively. *Fgf8* expression is less intense in the mutant. (D,D′) High magnification view of the tailbud region of embryos stained with brachyury; in the mutant staining of tailbud mesoderm at the tip appears fainter, but notochord (n) expression is unaffected. (E,E′) *Bmp4* expression in side view of 9.0 dpc embryos (after turning). The allantois (al) and lateral plate mesoderm (lpm) are stained. (F,F′) Higher magnification view of the tailbud region of embryos hybridized with *Bmp4*. The tailbud and of the allantois are abnormal in shape. Upon dissection, the allantois was found not to be fused to the chorion in the mutant (chorio-allantoic fusion has normally completed by this stage).

Martin, 1995) is also expressed in a transverse domain in the mutant instead of in two arches seen on each side of a wild-type embryo at 10.5 dpc (Fig. 7C-D′). These observations suggest that, as early as 9.5 dpc the hindlimb buds are fused in the ventral and posterior region. Expression of *Shh* in hindgut endoderm (Gofflot et al., 1997) was reduced in mutant embryos (Fig. 7E-F′), which confirms the reduction in hindgut structures observed in the histological analysis (Fig. 5E,E′ and see Fig. S2 in the supplementary material). Expression of *Shh* was normal in the notochord, but was delayed in the zone of polarizing activity (Fig. 7E-F′). In the tailbud, the number of cells expressing brachyury (Gofflot et al., 1997) at 9.5 dpc was reduced in ventral mesoderm but not in the notochord of mutant embryos (Fig. 7G-H′). We also note a ventral indentation continued posteriorly by a narrower tail in $Tsg^{-/-};Bmp7^{-/-}$ embryos (arrow in Fig. 7H′). We conclude that in mutant embryos the hindlimb bud territory is improperly specified as early as 9.5 dpc. The sirenomelia phenotype results from an early fusion of the posterior hindlimb buds that correlates with a deficit of ventral posterior mesoderm.

Discussion

Previous work has shown that *Tsg* is not essential for embryogenesis, as $Tsg^{-/-}$ mice are viable and fertile, but are smaller and exhibit skeletal defects (Nosaka et al., 2003; Petryk et al., 2004; Zakin and De Robertis, 2004). However, when one copy of *Bmp4* was removed in certain genetic backgrounds, *Tsg* was shown to exhibit a genetic interaction involved in forebrain formation (Zakin and De Robertis, 2004). As *Tsg* is broadly expressed throughout the embryo and many members of the *Bmp* family exist (Hogan, 1996; Zhao, 2003), we investigated whether genetic interactions with *Bmps* were a general feature of Tsg function by analyzing *Tsg;Bmp7* compound mutants. Our results show that in the absence of *Bmp7*, *Tsg* is required for the formation of posterior ventral structures.

Genetic interactions between *Tsg* and members of the *Bmp* family

Tsg interacts biochemically with Bmp4 (Oelgeschläger et al., 2000; Chang et al., 2001). In the mouse, Tsg interacts with Bmp4 in a dose-dependent fashion; in the absence of *Tsg*, the loss of one copy of *Bmp4* results in holoprosencephaly and branchial arch defects (Zakin and De Robertis, 2004). In the present study, we found that the combined functions of *Tsg* and *Bmp7* are required in a different aspect of embryogenesis. $Tsg^{-/-};Bmp7^{-/-}$ and $Tsg^{+/-};Bmp7^{-/-}$ compound mutants displayed sirenomelia. Embryonic lethality and sirenomelia were observed only in $Bmp7^{-/-}$ embryos in which one or two copies of *Tsg* were also missing. Thus, the dose of Tsg is the limiting factor. Tsg was shown to bind directly to Bmp7 (Fig. 1A) but could also interact with other Bmps, which could be functionally redundant to Bmp7 and compensate for its loss. When one copy of *Tsg* is removed in $Bmp7^{-/-}$ mutants, the levels of these other Bmp signals may fall beneath the

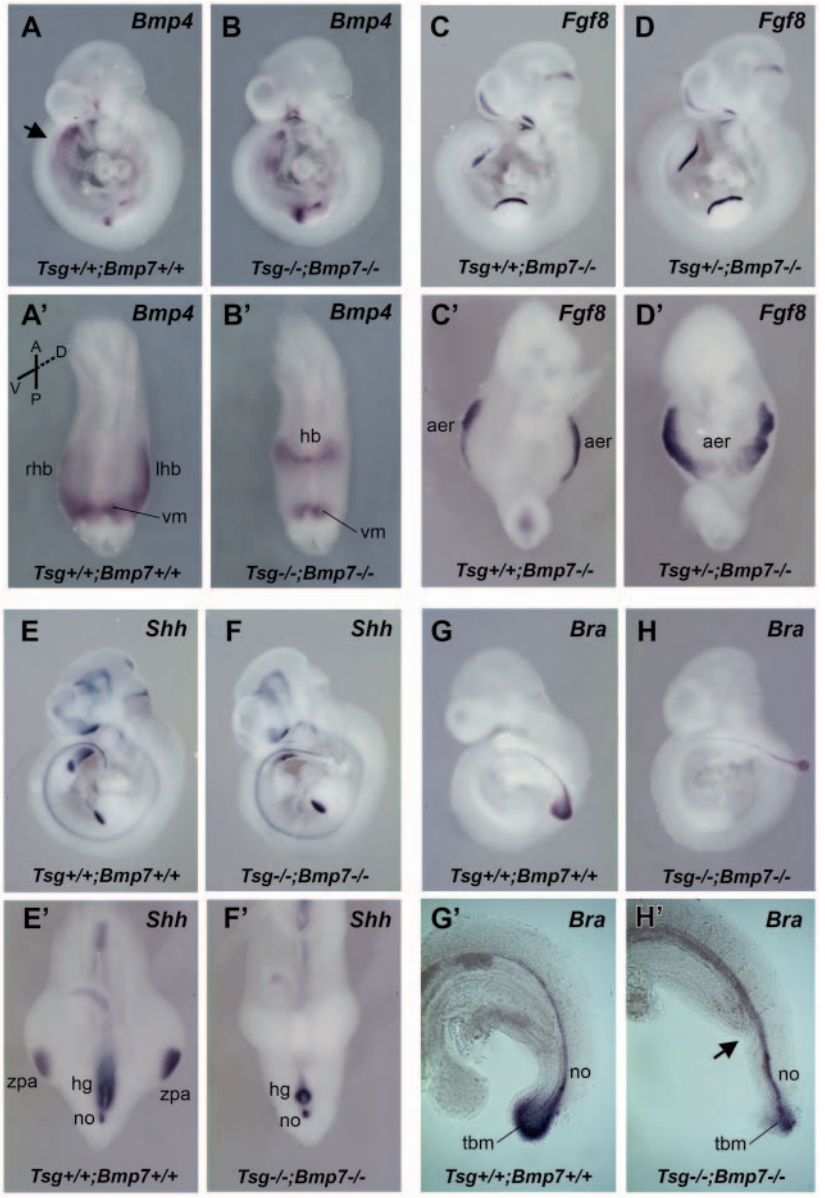

Fig. 7. Analysis of the sirenomelia phenotype. (A,B) Side view of 9.5 dpc wild-type and mutant embryos hybridized with *Bmp4* probe. (A′,B′) Ventral views of hindlimb bud region of embryos shown in A and B, respectively; the tail has been excised. In the mutant, expression of *Bmp4* in the future hindlimb bud mesoderm (hb) forms a transverse horizontal domain instead of two lateral ones on the right (rhb) and left (lhb) hindlimb buds seen in the wild type. (C,D) Side view of 10.5 dpc embryos hybridized with *Fgf8* probe, marking the apical ectodermal ridge (aer). (C′,D′) Ventral views of hindlimb bud region of embryos shown in C and D, respectively. In the mutant, the aer expression domain of *Fgf8* adopts a horseshoe-like shape, with the two aer regions meeting posteriorly instead of forming two lateral arches. (E,F) Side view of 10.5 dpc embryos hybridized with sonic hedgehog (*Shh*) probe. (E′,F′) Ventral views of hindlimb bud region at higher magnification. Expression of *Shh* in the zone of polarizing activity (zpa) is not yet detected, and hindgut (hg) staining is reduced in the mutant. (G,H) Side view of 9.5 dpc embryos hybridized with brachyury probe. (G′,H′) Higher magnification of tail region of embryos stained for brachyury. Staining of tail bud mesoderm (tbm) is decreased ventrally in the mutant; note the abnormal indentation (black arrow) and narrowing of the tail in the mutant. no, node; vm, ventral mesoderm.

threshold required for ventral mesoderm development. It is also possible that Bmp7 may actually modulate Tsg function; however, this seems unlikely in view of previous biochemical work showing that Tsg regulates the ability of Bmps to signal through Bmp receptors (Larrain et al., 2001; Oelgeschläger et al., 2003a).

One candidate for *Bmp7* compensation is *Bmp4*, as both *Bmp7* and *Bmp4* are expressed in ventroposterior mesoderm (Lawson et al., 1999) and *Bmp4* is required for tailbud formation in the frog (Beck et al., 2001). In mouse, *Bmp4;Bmp7* double heterozygotes display increased defects in the rib cages and limbs, supporting a cooperation between *Bmp4* and *Bmp7* (Katagiri et al., 1998). In addition, tetraploid chimeras lacking *Bmp4* in inner cell mass derivatives have impaired allantois differentiation, absence of the vitelline artery at 8.25 dpc and kinked neural tubes (Fujiwara et al., 2001). Because similar phenotypes are seen in our sirenomelic mutants, the defects observed could be the result of a deficit in Bmp4 activity. Another candidate for an interaction with Tsg is Bmp5. Embryonic lethality is observed in *Bmp5;Bmp7* double mutants but not in each individual mutant (Solloway and Robertson, 1999), and they display, among other defects, failure of chorioallantoic fusion and kinked neural tubes (Solloway and Robertson, 1999), also seen in our siren mutants.

Tsg and *Bmp7* are involved in posterior ventral mesoderm formation

When Tsg-MO and Bmp7-MO were co-injected into frog embryos, the loss of ventral fin and of tail structures was observed (Fig. 3). In *Xenopus*, the ventral mesoderm has been shown to be required for ventral fin formation (Tucker and Slack, 2004). In zebrafish, the loss of ventral fin is associated with decreased Bmp signaling (Bauer et al., 2001; Hammerschmidt and Mullins, 2002). For example, in the *mini fin* mutants, increased Bmp inhibition by Chd occurs, because Tolloid, the metalloprotease that cleaves Chd, is mutated (Connors et al., 1999). Moreover, knockdown of *Tsg* in zebrafish results in dorsalization consistent with a loss of Bmp signaling, and a genetic interaction between *swirl* (*Bmp2b*) and *Tsg* loss-of-function was observed; thus, Tsg functions in zebrafish to promote Bmp signaling in dorsoventral patterning (Little and Mullins, 2004; Xie and Fisher, 2005). In *Xenopus*, ventral mesodermal explants co-injected with Tsg-MO and Bmp7-MO become dorsalized (anti-Bmp phenotype) in a dose-dependent way (Fig. 4). Thus, as in zebrafish, but unlike other reports (Ross et al., 2001; Blitz et al., 2003), the function of Tsg protein in the *Xenopus* embryo is to promote the formation of ventral mesoderm by increasing the activity of Bmp7 and other Bmps.

In the mouse a loss of ventral mesoderm is also observed:

sirenomelia in *Tsg*$^{-/-}$;*Bmp7*$^{-/-}$ and *Tsg*$^{+/-}$;*Bmp7*$^{-/-}$ compound mutants is characterized by a reduction of *Fgf8* staining at 8.25 dpc, deficiencies of posterior lateral plate mesoderm expressing *Bmp4*, and a reduction of tail bud mesoderm expressing brachyury at 8.5 dpc. In tetraploid chimeras that lack *Bmp4* in the inner cell mass, a reduction of *Fgf8* in the primitive streak has been reported (Fujiwara et al., 2001). That study showed that extra-embryonic *Bmp4* was required for survival and differentiation of the allantois.

Mutations in the retinoic acid degrading enzyme *Cyp26* cause sirenomelia (Abu-Abed et al., 2001; Sakai et al., 2001). They differ from our *Tsg*$^{-/-}$;*Bmp7*$^{-/-}$ and *Tsg*$^{+/-}$;*Bmp7*$^{-/-}$ sirens in that they also display severely truncated tails and spina bifida. *Cyp26* knockouts showed a reduction of *Wnt3a* and brachyury expression, associated with impaired mesoderm proliferation and the mesoderm adopting neural fates (Sakai et al., 2001). In our mutants, we did not observe changes in the expression of *Wnt3a* nor excessive neural structures, but a reduced number of cells expressing brachyury in the tailbud mesoderm was seen. Preliminary results indicate that cell proliferation was not significantly changed, but apoptosis was increased in ventral posterior regions in compound mutants (L.Z. and E.M.D.R., unpublished). In the mouse, other work has implicated low Bmp signaling both in decreased cell proliferation and/or increased apoptosis (Solloway and Robertson, 1999; Fujiwara and Hogan, 2001). Although sirenomelia has variable phenotypic traits and multiple causes (Wei and Sulik, 1996; Padmanabhan, 1998), its occurrence is always associated with defects in posterior primitive streak. The sirenomelia phenotype observed here is consistent with a defective differentiation of the posterior and ventral mesoderm caused by decreased Bmp signaling.

A link between *Tsg*, *Bmp7* and the original sirens?

Sirens were discovered in the mouse (Gluecksohn-Schoenheimer and Dunn, 1945) among the progeny of parents carrying various combinations of the *Short-tail* (*T* locus), *anury* (t^0), *Fused* and *ur* mutations. The siren pups obtained had no tail, various degrees of reduction and fusion of elements of the hindlimbs, abnormalities of the spine, and fusion of ribs. Even though *Tsg*$^{-/-}$;*Bmp7*$^{-/-}$ and *Tsg*$^{+/-}$;*Bmp7*$^{-/-}$ sirenomelic pups do form tails (albeit shorter), the limb bud phenotypes we observe are very similar to those of Gluecksohn-Schoenheimer and Dunn. Could the old and new mutations be linked in any way? We note that the *T* locus (including brachyury), *Fused* (corresponding to *Axin*) (Zeng et al., 1997) and *Tsg* are all located on chromosome 17. The *us* mutation (urogenital syndrome) (Lyon and Searle, 1989), which is phenotypically identical to the now extinct *ur* (urogenital) mutant, and *Bmp7* are both located on chromosome 2. Although the respective locations of these genes on these chromosomes are distant from each other, mutations at the *T* locus correspond to important chromosomal rearrangements, often leading to duplications and deficiencies of chromosome segments upon cell division (Gluecksohn-Schoenheimer and Dunn, 1945). Thus, it is conceivable, although perhaps unlikely, that the occurrence of sirens in the initial description was associated with disruptions of the *Tsg* and/or *Bmp7* genes. Unfortunately, some of the original mutations have been lost, so this is not a testable proposition.

In subsequent work, Hoornbeek found sirenomelic neonates in crosses between SM/J and BUA strains studied for the incidence of the 'careener' phenotype (Hoornbeek, 1970; Schreiner and Hoornbeek, 1973). These sirens have the same phenotype as ours (fused hindlimbs, a tail, an abnormal umbilical artery). The genes affected in these crosses are not known, but the carriers of the 'siren' mutation (Hoornbeek, 1970) had tightly twisted tails, which is of relevance because *Tsg*$^{-/-}$ or *Bmp7*$^{-/-}$ mutants also have kinked tails (Jena et al., 1997; Zakin and De Robertis, 2004).

In conclusion, in the absence of *Bmp7*, two copies of *Tsg* are required for the proper differentiation of ventral and posterior structures. In the mouse, when Tsg and Bmp7 are mutated, the siren phenotype results from the fusion of the limb buds in the ventroposterior midline owing to a paucity of posterior ventral mesoderm. In *Xenopus*, knockdown of *Tsg* and *Bmp7* results in an analogous phenotype: loss of posteroventral cell fates associated with decreased Bmp activity. These results demonstrate a common mechanism, mediated by Bmp signaling, in mouse and frog in the patterning of the dorsoventral axis.

We thank A. Mays, D. Greenberg and D. Geissert for technical assistance. The probes used were kind gifts from B. Hogan, A. McMahon, G. Martin and R. Nusse. This work was supported by the Norman Sprague chair and the Howard Hughes Medical Institute, of which L.Z. is an Associate and E.M.D.R. an Investigator.

Supplementary material

Supplementary material for this article is available at
http://dev.biologists.org/cgi/content/full/132/10/2489/DC1

References

Abu-Abed, S., Dolle, P., Metzger, D., Beckett, B., Chambon, P. and Petkovich, M. (2001). The retinoic acid-metabolizing enzyme, CYP26A1, is essential for normal hindbrain patterning, vertebral identity, and development of posterior structures. *Genes Dev.* **15**, 226-240.

Ahn, K., Mishina, Y., Hanks, M. C., Behringer, R. R. and Crenshaw, E. B., 3rd (2001). BMPR-IA signaling is required for the formation of the apical ectodermal ridge and dorsal-ventral patterning of the limb. *Development* **128**, 4449-4461.

Bauer, H., Lele, Z., Rauch, G. J., Geisler, R. and Hammerschmidt, M. (2001). The type I serine/threonine kinase receptor Alk8/Lost-a-fin is required for Bmp2b/7 signal transduction during dorsoventral patterning of the zebrafish embryo. *Development* **128**, 849-858.

Beck, C. W., Whitman, M. and Slack, J. M. (2001). The role of BMP signaling in outgrowth and patterning of the Xenopus tail bud. *Dev. Biol.* **238**, 303-314.

Belo, J. A., Leyns, L., Yamada, G. and de Robertis, E. M. (1998). The prechordal midline of the chondrocranium is defective in Goosecoid-1 mouse mutants. *Mech. Dev.* **72**, 15-25.

Blitz, I. L., Cho, K. W. and Chang, C. (2003). Twisted gastrulation loss-of-function analyses support its role as a BMP inhibitor during early Xenopus embryogenesis. *Development* **130**, 4975-4988.

Chang, C., Holtzman, D. A., Chau, S., Chickering, T., Woolf, E. A., Holmgren, L. M., Bodorova, J., Gearing, D. P., Holmes, W. E. and Brivanlou, A. H. (2001). Twisted gastrulation can function as a BMP antagonist. *Nature* **410**, 483-487.

Collavin, L. and Kirschner, M. W. (2003). The secreted Frizzled-related protein Sizzled functions as a negative feedback regulator of extreme ventral mesoderm. *Development* **130**, 805-816.

Connors, S. A., Trout, J., Ekker, M. and Mullins, M. C. (1999). The role of tolloid/mini fin in dorsoventral pattern formation of the zebrafish embryo. *Development* **126**, 3119-3130.

Crossley, P. H. and Martin, G. R. (1995). The mouse Fgf8 gene encodes a family of polypeptides and is expressed in regions that direct outgrowth and patterning in the developing embryo. *Development* **121**, 439-451.

De Robertis, E. M. and Kuroda, H. (2004). Dorsal-ventral patterning and neural induction in Xenopus embryos. *Annu. Rev. Cell Dev. Biol.* **20**, 285-308.

Draper, B. W., Stock, D. W. and Kimmel, C. B. (2003). Zebrafish fgf24 functions with fgf8 to promote posterior mesodermal development. *Development* **130**, 4639-4654.

Dudley, A. T., Lyons, K. M. and Robertson, E. J. (1995). A requirement for bone morphogenetic protein-7 during development of the mammalian kidney and eye. *Genes Dev.* **9**, 2795-2807.
Eldar, A., Dorfman, R., Weiss, D., Ashe, H., Shilo, B. Z. and Barkai, N. (2002). Robustness of the BMP morphogen gradient in Drosophila embryonic patterning. *Nature* **419**, 304-318.
Feller, A. and Sternberg, H. (1931). Zur Kenntnis der Fehlbildungen der Wirbersaule. *Virchows Arch.* **280**, 649-692.
Fujiwara, T., Dunn, N. R. and Hogan, B. L. (2001). Bone morphogenetic protein 4 in the extraembryonic mesoderm is required for allantois development and the localization and survival of primordial germ cells in the mouse. *Proc. Natl. Acad. Sci. USA* **98**, 13739-13744.
Geoffroy Saint-Hilaire, I. (1837). Des monstres symeliens. In *Histoire generale et particuliere des anomalies de l'organisation chez l'homme et les animaux* (ed. J. B. Bailliere), pp. 237-264. Paris: Librairie de l'academie royale de medecine.
Gluecksohn-Schoenheimer, S. and Dunn, L. C. (1945). Sirens, aprosopi and intestinal abnormalities in the house mouse. *Anat. Rec.* **92**, 201-213.
Gofflot, F., Hall, M. and Morriss-Kay, G. M. (1997). Genetic patterning of the developing mouse tail at the time of posterior neuropore closure. *Dev. Dyn.* **210**, 431-445.
Graf, D., Timmons, P. M., Hitchins, M., Episkopou, V., Moore, G., Ito, T., Fujiyama, A., Fisher, A. G. and Merkenschlager, M. (2001). Evolutionary conservation, developmental expression, and genomic mapping of mammalian Twisted gastrulation. *Mamm. Genome* **12**, 554-560.
Hammerschmidt, M. and Mullins, M. C. (2002). Dorsoventral patterning in the zebrafish: bone morphogenetic proteins and beyond. *Results Probl. Cell Differ.* **40**, 72-95.
Heasman, J., Kofron, M. and Wylie, C. (2000). Beta-catenin signaling activity dissected in the early Xenopus embryo: a novel antisense approach. *Dev. Biol.* **222**, 124-134.
Henrique, D., Adam, J., Myat, A., Chitnis, A., Lewis, J. and Ish-Horowicz, D. (1995). Expression of a Delta homologue in prospective neurons in the chick. *Nature* **375**, 787-790.
Herrmann, B. G., Labeit, S., Poustka, A., King, T. R. and Lehrach, H. (1990). Cloning of the *T* gene required in mesoderm formation in the mouse. *Nature* **343**, 617-622.
Hogan, B. L. (1996). Bone morphogenetic proteins: multifunctional regulators of vertebrate development. *Genes Dev.* **10**, 1580-1594.
Hoornbeek, F. K. (1970). A gene producing symmelia in the mouse. *Teratology* **3**, 7-10.
Jena, N., Martin-Seisdedos, C., McCue, P. and Croce, C. M. (1997). BMP7 null mutation in mice: developmental defects in skeleton, kidney, and eye. *Exp. Cell Res.* **230**, 28-37.
Kampmeier, O. F. (1927). On sireniform monsters with a consideration of the causation and the predominance of the male sex among them. *Anat. Rec.* **34**, 365-389.
Katagiri, T., Boorla, S., Frendo, J. L., Hogan, B. L. and Karsenty, G. (1998). Skeletal abnormalities in doubly heterozygous Bmp4 and Bmp7 mice. *Dev. Genet.* **22**, 340-348.
Larrain, J., Oelgeschläger, M., Ketpura, N. I., Reversade, B., Zakin, L. and de Robertis, E. M. (2001). Proteolytic cleavage of Chordin as a switch for the dual activities of Twisted gastrulation in BMP signaling. *Development* **128**, 4439-4447.
Lawson, K. A., Dunn, N. R., Roelen, B. A., Zeinstra, L. M., Davis, A. M., Wright, C. V., Korving, J. P. and Hogan, B. L. (1999). Bmp4 is required for the generation of primordial germ cells in the mouse embryo. *Genes Dev.* **13**, 424-436.
Little, S. C. and Mullins, M. C. (2004). Twisted gastrulation promotes BMP signaling in zebrafish dorsal-ventral axial patterning. *Development* **131**, 5825-5835.
Lyon, M. F. and Searle, A. G. (1989). Genetic variants and strains of the laboratory mouse. Oxford: Oxford University Press.
Lyons, K. M., Hogan, B. L. and Robertson, E. J. (1995). Colocalization of BMP 7 and BMP 2 RNAs suggests that these factors cooperatively mediate tissue interactions during murine development. *Mech. Dev.* **50**, 71-83.
Mason, E. D., Konrad, K. D., Webb, C. D. and Marsh, J. L. (1994). Dorsal midline fate in Drosophila embryos requires twisted gastrulation, a gene encoding a secreted protein related to human connective tissue growth factor. *Genes Dev.* **8**, 1489-1501.
McMahon, J. A., Takada, S., Zimmerman, L. B., Fan, C. M., Harland, R. M. and McMahon, A. P. (1998). Noggin-mediated antagonism of BMP signaling is required for growth and patterning of the neural tube and somite. *Genes Dev.* **12**, 1438-1452.
Nosaka, T., Morita, S., Kitamura, H., Nakajima, H., Shibata, F., Morikawa, Y., Kataoka, Y., Ebihara, Y., Kawashima, T., Itoh, T. et al. (2003). Mammalian twisted gastrulation is essential for skeleto-lymphogenesis. *Mol. Cell. Biol.* **23**, 2969-2980.
Oelgeschläger, M., Larrain, J., Geissert, D. and de Robertis, E. M. (2000). The evolutionarily conserved BMP-binding protein Twisted gastrulation promotes BMP signalling. *Nature* **405**, 757-763.
Oelgeschläger, M., Reversade, B., Larrain, J., Little, S., Mullins, M. C. and de Robertis, E. M. (2003a). The pro-BMP activity of Twisted gastrulation is mediated by inhibition of Chordin-like BMP-binding modules. *Development* **130**, 4047-4056.
Oelgeschläger, M., Kuroda, H., Reversade, B. and de Robertis, E. M. (2003b). Chordin is required for the Spemann organizer transplantation phenomenon in Xenopus embryos. *Dev. Cell* **4**, 219-230.
Padmanabhan, R. (1998). Retinoic acid-induced caudal regression syndrome in the mouse fetus. *Reprod. Toxicol.* **12**, 139-151.
Petryk, A., Anderson, R. M., Jarcho, M. P., Leaf, I., Carlson, C. S., Klingensmith, J., Shawlot, W. and O'Connor, M. B. (2004). The mammalian twisted gastrulation gene functions in foregut and craniofacial development. *Dev. Biol.* **267**, 374-386.
Piccolo, S., Agius, E., Lu, B., Goodman, S., Dale, L. and de Robertis, E. M. (1997). Cleavage of Chordin by Xolloid metalloprotease suggests a role for proteolytic processing in the regulation of Spemann organizer activity. *Cell* **91**, 407-416.
Roelink, H. and Nusse, R. (1991). Expression of two members of the Wnt family during mouse development–restricted temporal and spatial patterns in the developing neural tube. *Genes Dev.* **5**, 381-388.
Ross, J. J., Shimmi, O., Vilmos, P., Petryk, A., Kim, H., Gaudenz, K., Hermanson, S., Ekker, S. C., O'Connor, M. B. and Marsh, J. L. (2001). Twisted gastrulation is a conserved extracellular BMP antagonist. *Nature* **410**, 479-483.
Sadler, T. W. and Langman, J. (2004). *Langman's Medical Embryology*. Baltimore, MD: Lippincott Williams and Wilkins.
Sakai, Y., Meno, C., Fujii, H., Nishino, J., Shiratori, H., Saijoh, Y., Rossant, J. and Hamada, H. (2001). The retinoic acid-inactivating enzyme CYP26 is essential for establishing an uneven distribution of retinoic acid along the anterio-posterior axis within the mouse embryo. *Genes Dev.* **15**, 213-225.
Schreiner, C. A. and Hoornbeek, F. K. (1973). Developmental aspects of sirenomelia in the mouse. *J. Morphol.* **141**, 345-358.
Scott, I. C., Blitz, I. L., Pappano, W. N., Maas, S. A., Cho, K. W. and Greenspan, D. S. (2001). Homologues of Twisted gastrulation are extracellular cofactors in antagonism of BMP signalling. *Nature* **410**, 475-478.
Solloway, M. J. and Robertson, E. J. (1999). Early embryonic lethality in Bmp5;Bmp7 double mutant mice suggests functional redundancy within the 60A subgroup. *Development* **126**, 1753-1768.
Sun, X., Meyers, E. N., Lewandoski, M. and Martin, G. R. (1999). Targeted disruption of Fgf8 causes failure of cell migration in the gastrulating mouse embryo. *Genes Dev.* **13**, 1834-1846.
Tucker, A. S. and Slack, J. M. (2004). Independent induction and formation of the dorsal and ventral fins in Xenopus laevis. *Dev. Dyn.* **230**, 461-467.
Wei, X. and Sulik, K. K. (1996). Pathogenesis of caudal dysgenesis/sirenomelia induced by ochratoxin A in chick embryos. *Teratology* **53**, 378-391.
Wilson, V., Manson, L., Skarnes, W. C. and Beddington, R. S. (1995). The T gene is necessary for normal mesodermal morphogenetic cell movements during gastrulation. *Development* **121**, 877-886.
Winnier, G., Blessing, M., Labosky, P. A. and Hogan, B. L. (1995). Bone morphogenetic protein-4 is required for mesoderm formation and patterning in the mouse. *Genes Dev.* **9**, 2105-2116.
Xie, J. and Fisher, S. (2005). Twisted gastrulation enhances BMP signaling through chordin dependent and independent mechanisms. *Development* **132**, 383-391.
Yoshikawa, Y., Fujimori, T., McMahon, A. P. and Takada, S. (1997). Evidence that absence of Wnt-3a signaling promotes neuralization instead of paraxial mesoderm development in the mouse. *Dev. Biol.* **183**, 234-342.
Zakin, L. and de Robertis, E. M. (2004). Inactivation of mouse Twisted gastrulation reveals its role in promoting Bmp4 activity during forebrain development. *Development* **131**, 413-424.
Zeng, L., Fagotto, F., Zhang, T., Hsu, W., Vasicek, T. J., Perry, W. L., 3rd, Lee, J. J., Tilghman, S. M., Gumbiner, B. M. and Costantini, F. (1997). The mouse Fused locus encodes Axin, an inhibitor of the Wnt signaling pathway that regulates embryonic axis formation. *Cell* **90**, 181-192.
Zhao, G. Q. (2003). Consequences of knocking out BMP signaling in the mouse. *Genesis* **35**, 43-56.